Supporting Information for "Robust Relationship Between Midlatitudes CAPE and Moist Static Energy Surplus in Present and Future Simulations"

Ziwei Wang [1,2], Elisabeth J. Moyer [1,2]

[1]Department of the Geophysical Sciences, University of Chicago, Chicago, Illinois

[2]Center for Robust Decision-making on Climate and Energy Policy (RDCEP), University of Chicago, Chicago, Illinois

Contents of this file

Text S1. Derivation of CAPE-MSE surplus framework

In this section we show the background for the framework in our manuscript. We repeat the derivation from Emanuel, *Atmospheric Convection* (1994) that restates CAPE as a function of pseudo-entropy, show how this can be approximated as a linear dependence in pseudo-enthalpy (moist static energy), and finally demonstrate that the error introduced by the core assumption required in Emanuel (1994) (hereafter E94) – that virtual temperature corrections can be ignored – is relatively minor and considerably smaller than that in an alternative CAPE framework.

Emanuel (1994) derivation

We start from the definition of CAPE in pressure coordinates:

$$CAPE = \int_{p_n}^{p_i} (\alpha_p - \alpha_a) dp \tag{1}$$

where α_p and α_a are the volume per mass for air in the parcel and the environment, respectively. Because CAPE is a positive quantity, the integration is from low to high pressure, i.e. from the top of a convective event (p_n) to the level of convective initiation (p_i).

The rising parcel will be saturated, and changes in its volume per mass can be divided into two terms, separating the effects of its saturation pseudo-entropy s^* (which is independent of moisture) and of its actual moisture content. That is:

$$\Delta\alpha = \left.\frac{\partial \alpha}{\partial s^*}\right|_r \Delta s^* + \left.\frac{\partial \alpha}{\partial r}\right|_{s^*} \Delta r \tag{2}$$

If we treat the environment as also saturated – acceptable if the effect of moisture on density is small – then it can be similarly decomposed and CAPE can be written as:

$$CAPE = \int_{p_n}^{p_i} \left(\frac{\partial \alpha}{\partial s^*}(s_p^* - s_a^*) + \frac{\partial \alpha}{\partial r}(r_p - r_a) \right) \cdot dp \tag{3}$$

The volume per mass of dry air (α_d) can be approximated as $\alpha_d = \frac{\alpha}{1+r}$. where r is the mass mixing ratio of water vapor, typically 0.01 or less. Emanuel then makes the further assumption that the buoyancy effects of this water vapor r (the virtual temperature effect) can be neglected entirely, so that the second term in Equation (3) vanishes and in the first term α is replaced by α_d. This yields Eq. (6.4.2a) in Emanuel (1994):

$$CAPE \approx \int_{p_n}^{p_i} \frac{\partial \alpha_d}{\partial s^*}(s_p^* - s_a^*) \cdot dp \tag{4}$$

The neglect of virtual temperature effects for both parcel and environment produces a slight net underestimation of derived CAPE, but the distortion is smaller than in other approximate CAPE frameworks and is compensated for by the empirical regression coefficient. See discussion at the end of the section and Figure S1. The Maxwell relationship $(\frac{\partial \alpha}{\partial s})_p = (\frac{\partial T}{\partial p})_s$ allows converting the integration coordinate in Equation (4) from pressure to temperature:

$$CAPE = \int_{p_n}^{p_i} \frac{\partial T}{\partial p}(s_p^* - s_a^*) \cdot dp \tag{5}$$

$$= \int_{T_n}^{T_i} (s_p^* - s_a^*) \cdot dT \tag{6}$$

which is Equation (6.4.2) in Emanuel (1994).

Because the integration is now over temperature, and the difference between environment and parcel is taken at the same T, we can readily substitute saturated pseudo-enthalpy h^* for the saturated pseudo-entropy s^* via:

$$\Delta h^* = T\Delta s* \tag{7}$$

Equation (6) then becomes:

$$CAPE = \int_{T_n}^{T_i} \frac{h_p^* - h_a^*}{T} dT \tag{8}$$

Here $h_p^* = h_s$ is conserved for an adiabatically rising parcel, while the moist static energy of the environment h_a^* is a weak function of T in individual atmospheric profiles, reaching a minimum in mid-troposphere that can be $<15\%$ below h_s.

Approximating the integral as a simple difference

All simplified frameworks for CAPE must replace the integral with some kind of simple difference. If the moist static energy difference between the parcel and the environment were independent of T, we could write

$$CAPE = (h_s - \overline{h^*}) \cdot ln\frac{T_i}{T_n} \tag{9}$$

This assumption is obviously not realistic and in practice the true shape of atmospheric profiles necessitates adding an empirical coefficient to the relationship. Since an empirical coefficient is needed regardless, for convenience we take the difference at the location of the minimum tropospheric MSE, typically around 650 mb.

$$CAPE \approx A \cdot (h_s - h_m^*) \tag{10}$$

which is the linear relationship used in this work; $(h_s - h_m^*)$ is the " MSE surplus". The coefficient A captures the shape of the profile, and, if virtual temperature corrections were indeed negligible, would be mathematically constrained to be between zero and $ln\frac{T_i}{T_n}$ (see also Agard and Emanuel (2017)), at maximum $\sim$0.4 (for $T_i = 300$ K, $T_n = 200$ K). (In practice, compensating for the neglected virtual temperature corrections raises A slightly.) For the same temperature range, a larger A corresponds to a more uniform Δh profile between the lifting condensation level and the tropopause. For the dataset used in this work, the empirical slope A is 0.27.

Effect of assumptions in derivation

The derivation in E94 relies on two successive assumptions about the direct effect of water on the density of the environment through which a parcel rises. We show here that the effect of these assumptions is not prohibitive and is smaller than the effect of the core assumption in the alternative CAPE framework of Eq. (5) in Li and Chavas (2021) (LC21). The assumptions are:

- E94a: compute the virtual temperature effect for the environment assuming saturation
- E94b: neglect the virtual temperature effect for both parcel and environment
- LC21 Equation (5): assume all water vapor in the parcel condenses at the LCL

In reality, the mean environmental relative humidity in our high-CAPE midlatitudes summertime profiles is 0.44 (for all levels below 200 hPa). Both of the assumptions in E94 will therefore produce an underestimation of CAPE (the parcel is less buoyant than in reality), while that in LC21 will produce an overestimation (the parcel is more buoyant).

We illustrate the effects of these assumptions on an example atmospheric profile in Figure S1. The example profile is chosen to match the location and time of Figure 3 in Li and Chavas (2021): Springfield, MO in early June. At 650 hPa, the true buoyancy $g\frac{\Delta T_v}{T_{ve}}$ is 0.143 m/s^2. The assumptions in E94 underestimate buoyancy by 14% and 22% (0.123 and 0.111 m/s^2), while that in LC21 overestimates it by a factor of 6 (0.845 m/s^2). The discrepancies are about half as large when averaged over the parcel's ascent but their relative sizes are unchanged: E94a,b cause underestimations of 6% and 7% and LC21 causes an overestimation of a factor of 3. If we use instead an average summertime profile over the Southeastern U.S., the bias produced by E94 remains below 13% while that in LC21 is a factor of eight. In both frameworks, the bias is largely accounted for by an empirical regression coefficient, but the more modest assumptions of E94 lead to a robust regression across climate states.

References

Agard, V., & Emanuel, K. (2017). Clausius–Clapeyron scaling of peak CAPE in continental convective storm environments. *Journal of the Atmospheric Sciences*, *74*(9), 3043–3054.

Emanuel, K. (1994). Atmospheric Convection, Chap. 6. In (pp. 169–175). Oxford Univ. Press.

Li, F., & Chavas, D. R. (2021). Midlatitude continental CAPE is predictable from large-scale environmental parameters. *Geophysical Research Letters*, *48*(8), e2020GL091799.

Figures S1 – S9

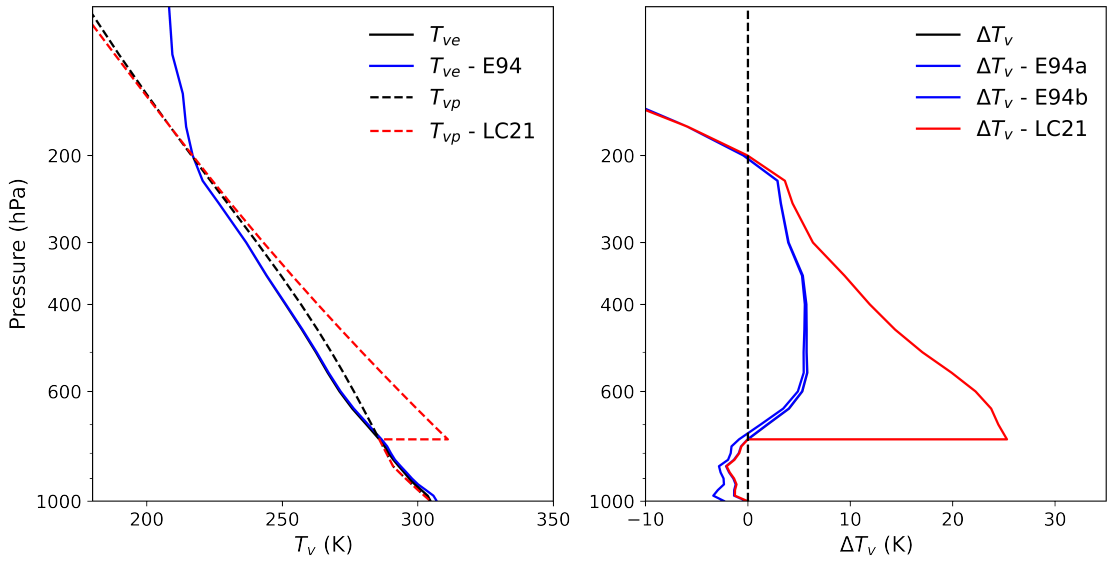

Figure S1. Illustration of the effect of assumptions in E94 and LC21, on (left) the virtual temperatures of parcel and environment and (right) the virtual temperature difference between parcel and environment. The example profile is that for a 1 $\times$ 1 deg grid in ERA5 including Springfield, MO, at 18 UTC on June 6th, 2005, chosen to approximately match the snapshot used in LC21 Figure 3 (0000 UTC June 07, 2011). E94a (green) raises the environmental T_v; E94b (blue) lowers T_v in both environment and parcel; and LC21 (red) raises T_v in the parcel by condensing all water at the LCL. The biases introduced by E94 are more modest than those in LC21, though all are ultimately accounted for by empirical regression coefficients.

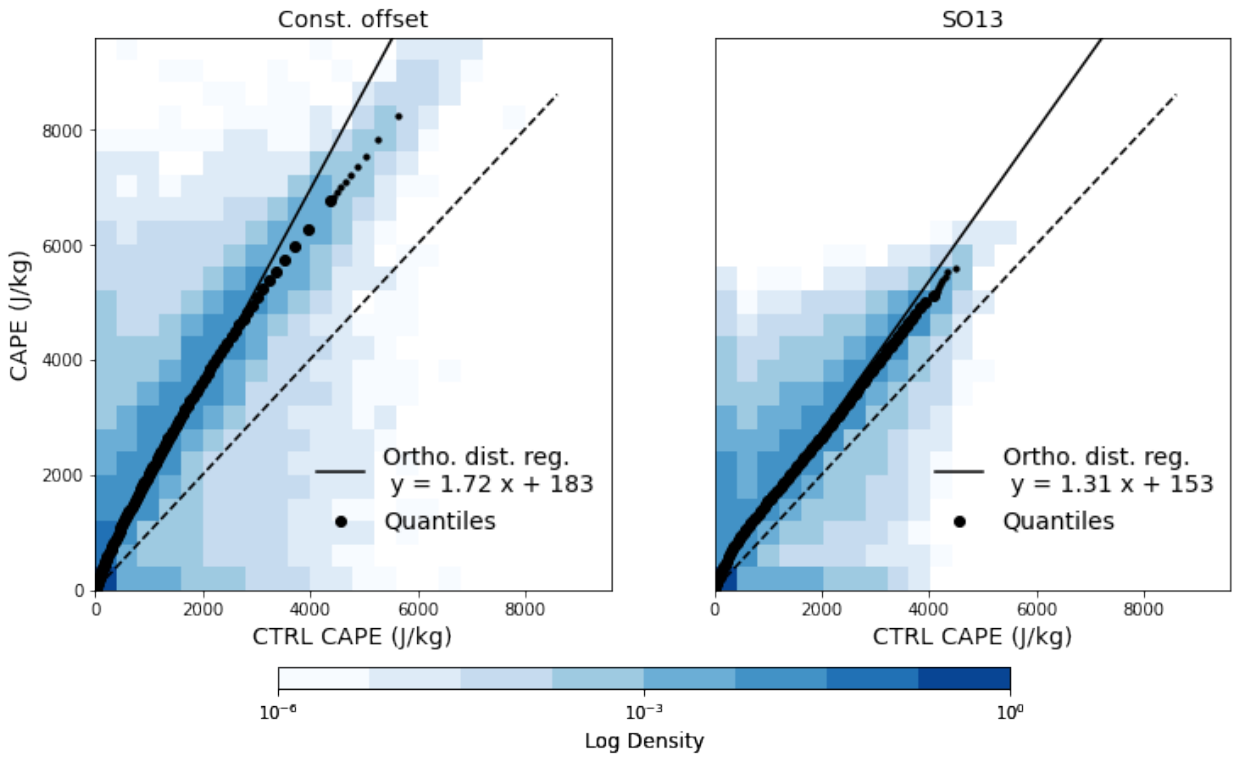

Figure S2. Changes between present and future CAPE, as in main text Figure 1 left panel, but for (left) *constant-offset* and (right) *SO13*, calculated as described in text. CAPE changes are too large in *constant offset* and too small in *SO13*: dividing by 4.65 K produces fractional changes of 12%/K and 6%/K, respectively, vs. the 8%/K derived from model output. For *constant offset* in particular, the quantiles fall below the orthogonal distance regression line above the 80th percentile. In both cases, however, the quantile regression matches the orthogonal distance regression reasonably well.

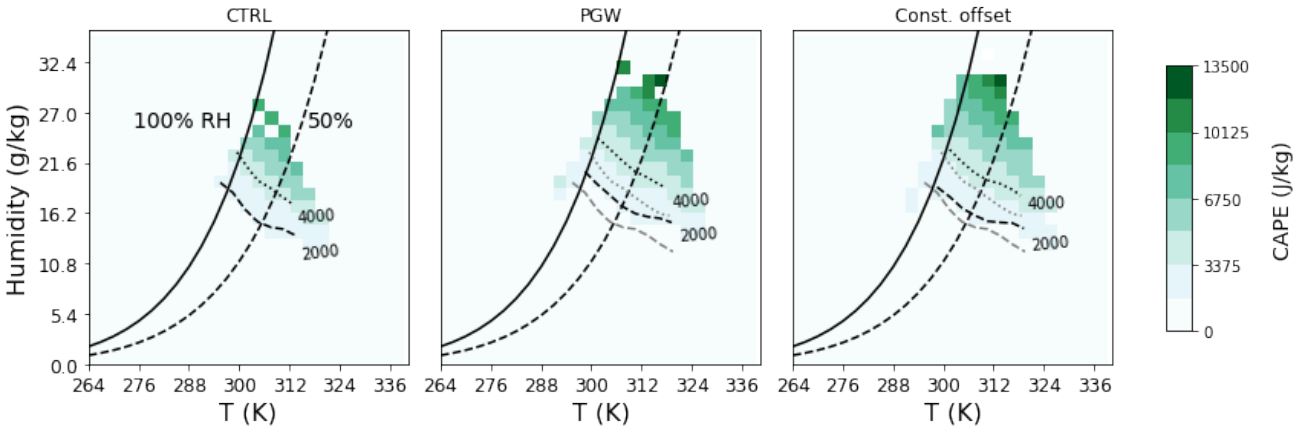

Figure S3. (Left and middle) Mean CAPE heatmap as in main text Figure 2 for present and future model output and (right) for the *constant offset* synthetic representation of future CAPE. Contours in black show CAPE of 2000 and 4000 J/kg in each panel, with CTRL contours repeated in gray in middle and right panels. Contours shift in PGW model output (center), meaning that warmer or wetter conditions are required to achieve the same CAPE. The *constant offset* synthetic (right), which involves changes in surface conditions alone and has no lapse rate adjustment, exhibits about half the shift of the PGW simulations.

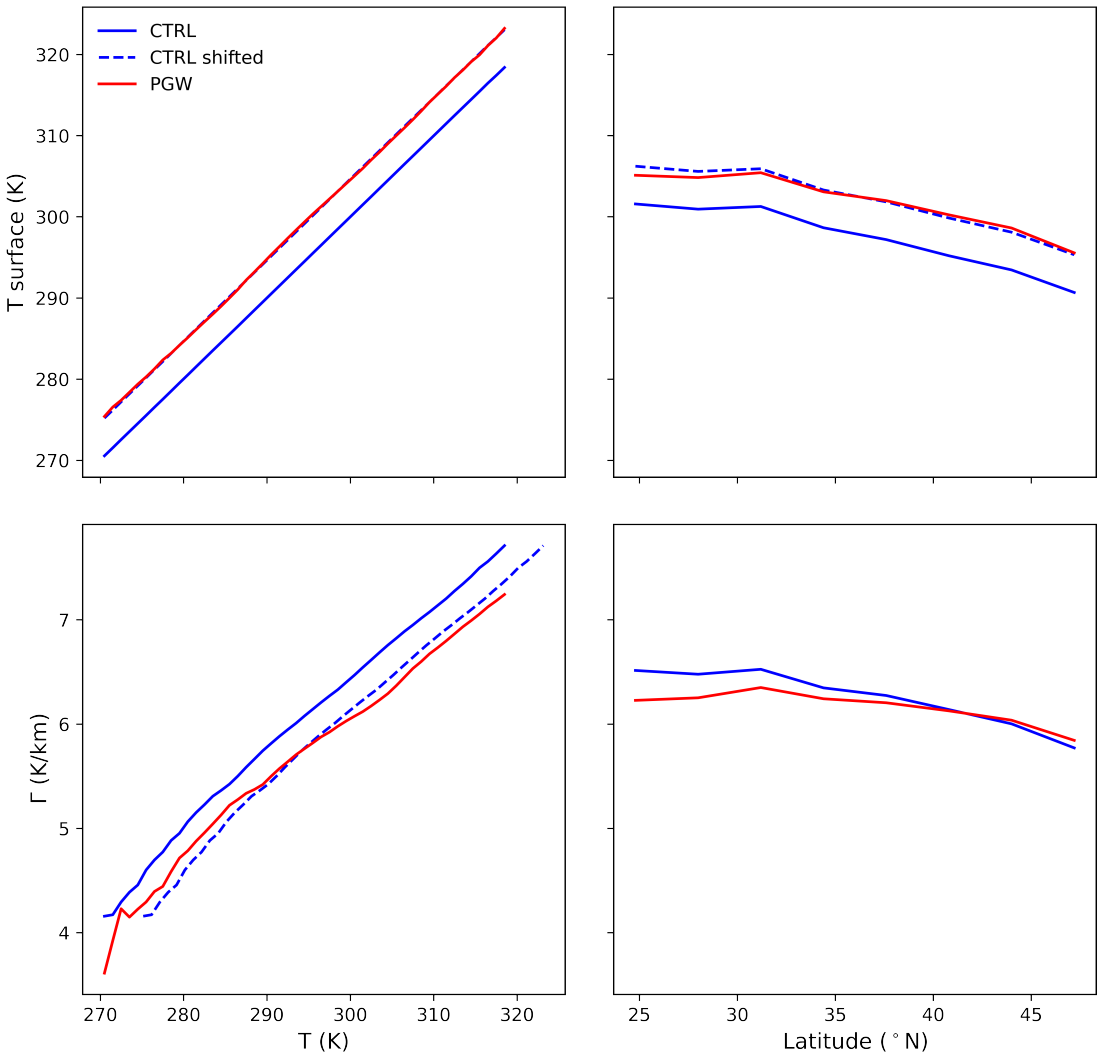

Figure S4. Changes in (top) temperature and (bottom) lapse rate as a function of (left) temperature bins and (right) latitudinal bins. The blue dashed lines are synthetics applying a same 4.65 K offset to the CTRL climate (blue solid lines). The damping of CAPE under a warmer climate can be explained by a more stable lapse rate associated with a given set of surface conditions.

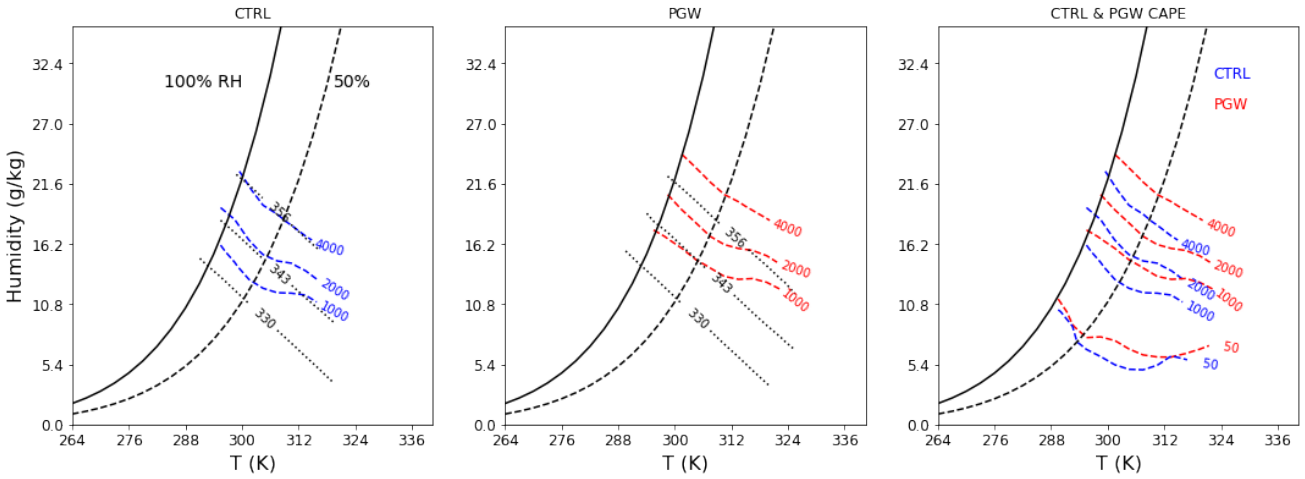

Figure S5. Contours of CAPE and surface moist static energy (MSE) in model output for simulations in present (CTRL, left) and future (PGW, middle) conditions. CAPE contours follow those of moist static energy in the convection-promoting regime (CAPE $>$ 1000 J/kg, RH $>$ 40%), The relationship differs between CTRL and PGW (right). Contours here are cut off at RH=100%, as in main text Figure 2. CAPE contours aligns with those of surface MSE in conditions with high CAPE, suggesting a strong dependence between CAPE and surface MSE. Future changes in CAPE can be translated to a change in mapping between surface MSE and CAPE.

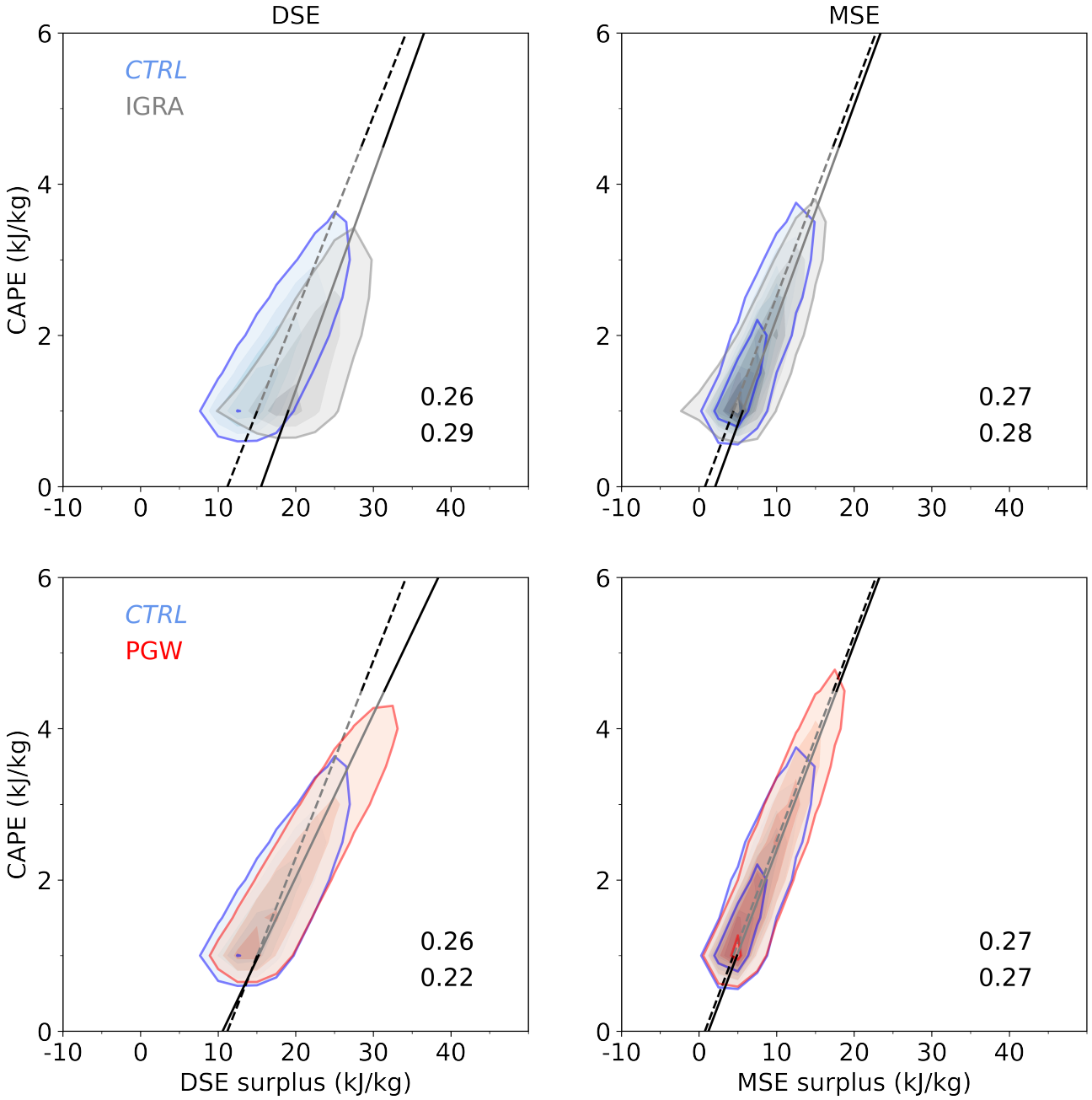

Figure S6. Comparison of the CAPE relationship with dry static energy (DSE) surplus (left) and with MSE surplus (right). DSE surplus is defined as the difference between surface MSE and mean mid-tropospheric DSE (virtual-temperature weighted free troposphere DSE). The top rows show model output (WRF) versus observations (IGRA) under CTRL climate, and the bottom rows show CTRL versus PGW in model output. Color shading increments are 1.5% for all panels, and the text shows the slopes for CTRL and IGRA/PGW. Conclusions are 1) the WRF simulation realistically reproduces the observed joint distribution of CAPE and MSE surplus and 2) a linear expression with MSE surplus outperforms that with DSE surplus both in residual variance and in robustness.

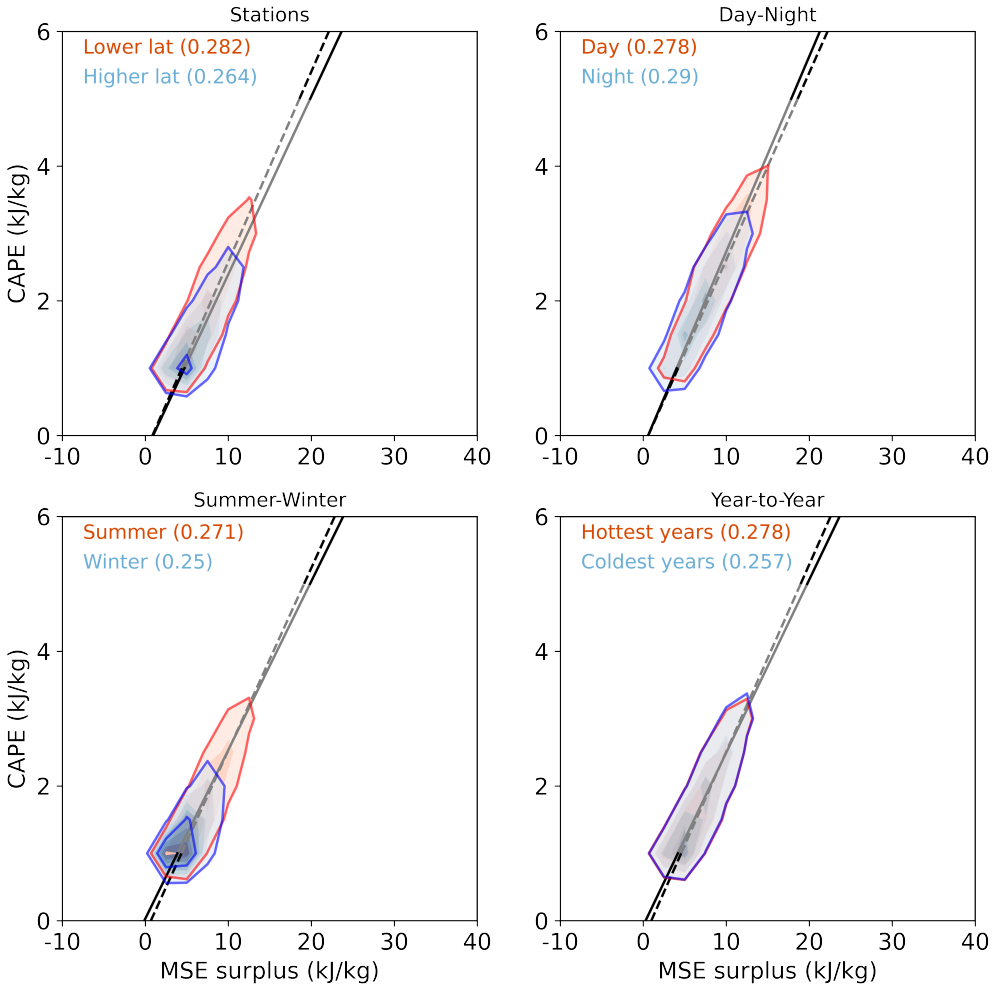

Figure S7. Tests of the robustness of the CAPE-MSE surplus relationship with different subsets of the data. *Top left*: stations lower and higher latitude than 35N. *Top right*: daytime versus nighttime (using only stations below 30N, to avoid biasing the sampling). *Bottom left*: summertime (MJJA) versus wintertime (NDJF) (all other panels use summertime data only; note that the month of February 2005 in the PGW run is removed due to missing surface 2D fields). *Bottom right*: the hottest 3 years (2001, 2006, 2012) versus the coldest 3 years (2004, 2008, 2009). Figure uses only CAPE $\geq$ 1000 J/kg, and all panels besides lower L. use summertime data only. MSE surplus is derived using the minimum saturation MSE in each individual profile. Each color shading is a 1.5% increment in density, and the orthogonal regression is fit using binned median values. The CAPE-MSE surplus framework (including its intercepts and slopes) is highly consistent across all cases tested.

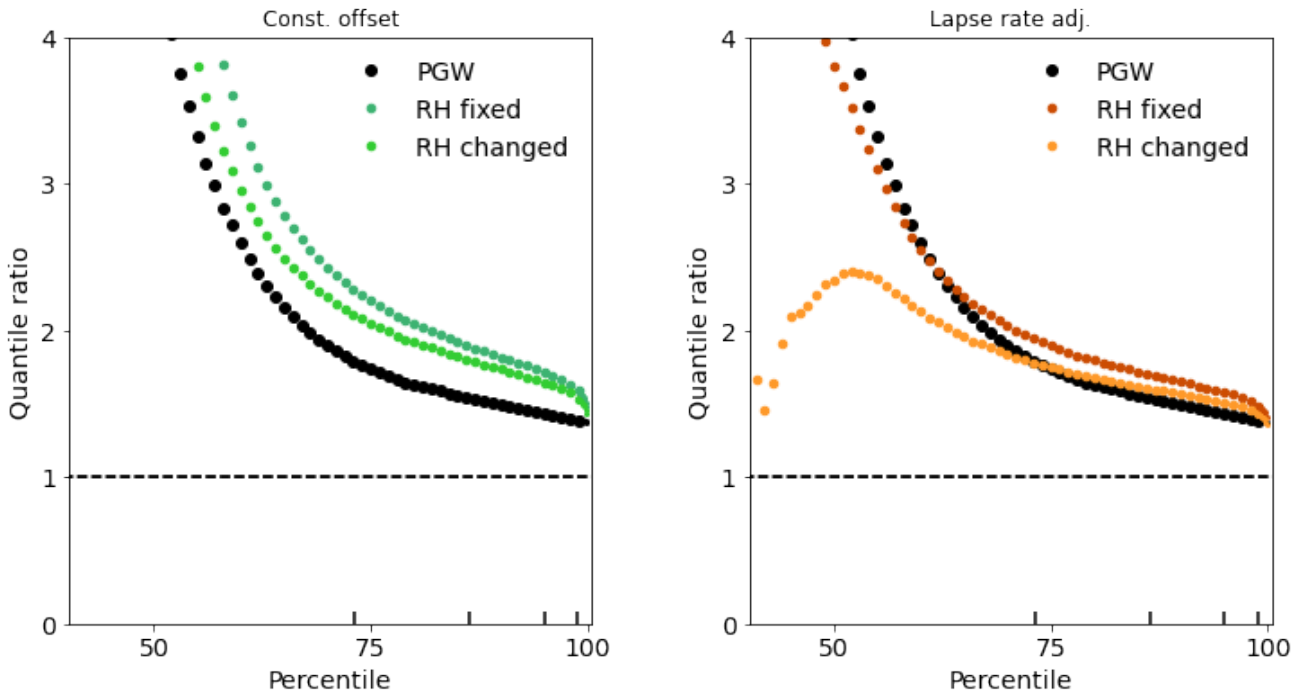

Figure S8. Quantile ratio plots of future–present CAPE in model output (PGW vs. CTRL) and in synthetic future distributions, showing also the effect of RH changes. For each synthetic we show one version with constant surface RH and one with a uniform $\sim$1% reduction, which lowers future CAPE changes by about 6% in both cases. (Left) *Constant offset*. Mean fractional changes are 1.92 with fixed RH and 1.81 with the reduction. Values are derived from the average quantile ratios for $\geq$ 73rd percentile. (Right) *Lapse rate adjustment*. Mean fractional changes are 1.71 and 1.61.

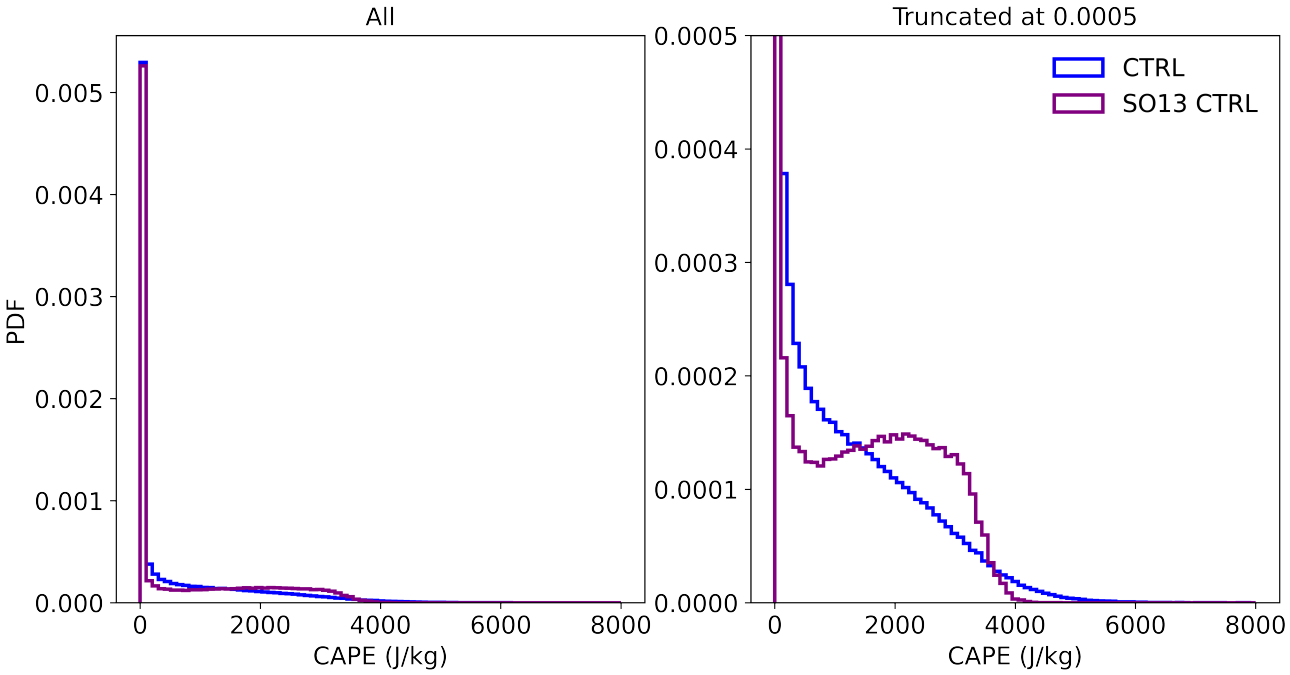

Figure S9. Comparison of probability distributions of midlatitdues summertime CAPE under current CTRL climate in our WRF model output and in the SO13 zero-buoyancy model driven by CTRL surface temperatures. (Left) full CAPE distribution and (right) with y-axis truncated at 0.0005 to show detail. The zero-buoyancy model cannot reproduce a realistic distribution, overestimating the occurrence of moderately high CAPE (between 1500 and 3500 J/kg). This peak occurs even though we modify the SO13 procedure to force the integration to stop at the actual LNB of each profile. Without that modification, SO13 cannot produce zero-CAPE values and the distribution is even more unimodal. SO13 is designed to reproduce climatological means in strongly convecting regions and is not appropriate for midlatitudes land.

Tables S1 – S2

Table S1. List of CMIP6 Models included in this study and shown in main text Figure 3. The outputs are 6-hourly model level data, for both *historical* and *ssp585* experiments. All model output is available from ESGF (`https://esgf-node.llnl.gov/search/cmip6/`).

Model	Variant label	Horizontal grid	Vertical levels
ACCESS-ESM1-5	r6i1p1f1	192 × 145	38
CanESM5	r1i1p2f1	128 × 64	49
CMCC-CM2-SR5	r1i1p1f1	288 × 192	30
CNRM-CM6-1	r1i1p1f2	256 × 128	91
CNRM-ESM2-1	r1i1p1f2	256 × 128	91
EC-Earth3	r1i1p1f1	512 × 256	91
GISS-E2-1-G	r1i1p1f2	144 × 90	40
MIROC-ES2L	r1i1p1f2	128 × 64	40
MPI-ESM1-2-LR	r1i1p1f1	192 × 96	47
MPI-ESM1-2-HR	r1i1p1f1	384 × 192	95
NorESM2-MM	r1i1p1f1	288 × 192	32

Table S2. Evaluating synthetics: fitted slopes and intercepts of the future CAPE-MSE framework as in main text Figure 4, for actual PGW model output and for three synthetic datasets. *C–C* scaling produces too small a slope and *constant offset* too small an intercept. *Lapse rate adjustment* performs well at both.

	PGW	C–C	Constant offset	Lapse rate adj.
slope	0.239	0.271	0.240	0.236
x-intercept (kJ/kg)	346.2	350.4	343.8	345.8